Automatic feedback control for resource-aware characterisation of genetic circuits

Kirill Sechkar
Department of Engineering Science
University of Oxford
Oxford, UK
kirill.sechkar@queens.ox.ac.uk

Harrison Steel*
Department of Engineering Science
University of Oxford
Oxford, UK
harrison.steel@eng.ox.ac.uk

***Abstract*—Many applications of engineered cells are enabled by genetic circuits – networks of genes regulating each other to process stimuli. Complex circuits are built by combining standardised modular components with different functions. Nonetheless, genes within a cell compete for the same limited pool of cellular resources, causing unintended interactions that violate modularity. Circuit components therefore behave differently when combined versus when observed in isolation, which can compromise a biotechnology's predictability and reliability. To forecast steady-state interactions between modules, experimental protocols for characterising their resource competition properties have been proposed. However, they rely on open-loop batch culture techniques in which dynamic control signals cannot be applied to cells. Consequently, these experimental methods have limited predictive power since they may fail to capture all possible steady states, such as repelling equilibria that would not be approached by an unsteered system. In contrast, we present the blueprint for a novel, comprehensive protocol for characterising the resource-dependence of genetic modules' performance. Based on the control-based continuation technique, it captures both stable and unstable steady states by applying stabilising cybergenetic feedback with an automated cell culturing platform. Using a range of models with different degrees of complexity, we simulate applying our pipeline to a self-activating genetic switch. This case study illustrates how informative characterisation of a genetic module with automatic feedback control can enable reliable forecasting of its performance when combined with any other circuit component. Hence, our protocol promises to restore predictability to the design of genetic circuits from standardised components.**

***Index Terms*—Synthetic Biology, Genetic Expression, Bifurcation, Feedback, Automatic Control, Mathematical Models**

I. Introduction

A. Challenges of resource-aware circuit characterisation

Emerging applications of engineered cells as biosensors, biomanufacturing platforms, and living therapeutics are powered by gene circuits – networks of genes that regulate each other to perceive, process and react to complex stimuli [1], [2]. The engineering principles of modularity and standardisation allow to construct increasingly sophisticated circuits by combining genetic modules with different functions [3]. However, all genes within a cell compete for the same limited pool of expression resources – such as ribosomes – which introduces unintended indirect interactions between a circuit's components. Due to these indirect resource couplings, genetic modules behave differently when joined into a circuit compared to when they are characterised in isolation, which can compromise the predictability and reliability of biotechnologies' performance [2], [4].

This predictability challenge has given rise to a range of resource-aware mathematical models of gene expression, which incorporate resource coupling dynamics into their ordinary differential equations (ODEs) [1], [2], [5], [6]. However, these models' predictions are contingent on knowing a system's parameters, whose estimation from experimental data involves significant uncertainty and may be expensive and time-consuming [7]. Alternatively, instead of inferring all model parameters, experiments can be designed to measure lumped factors capturing a genetic module's empirically observed input-output relationships, which can be reproduced by many different modelling frameworks [1], [4]. This allows to forecast resource competition between any two genetic modules for which these quantities are known. For instance, McBride and Del Vecchio suggested predicting steady-state circuit behaviours based on 'resource demand' factors, measured for each genetic module of interest by observing cells which express it alongside a constitutive (i.e. unregulated) reporter gene with previously characterised resource competition properties (Fig. 1a) [4].

However, such open-loop experimental methods – like characterising a module using constitutive reporters whose resource demands remain fixed over time – may only observe one among many possible equilibria of a system (Fig. 1a) [7], [8]. At the same time, multistability is a key feature of gene regulatory networks and is suggested to underlie cellular development and adaptability to environmental changes in nature [3], [9], as well as being observed in synthetic gene circuits [3], [7], [10]. Lack of insights into multistability is a key limitation for observing resource couplings, as competition may not only shift a circuit's equilibria [2], [4], but also cause bifurcations that qualitatively alter their number and identity [3], [11]. These bifurcations, for instance, have been leveraged by a biomolecular controller improving biotechnologies' robustness to mutations [12]. Meanwhile, observing a system's

*Corresponding author.
This work was supported in part by Engineering and Physical Sciences Research Council (EPSRC) project EP/Y014073/1.

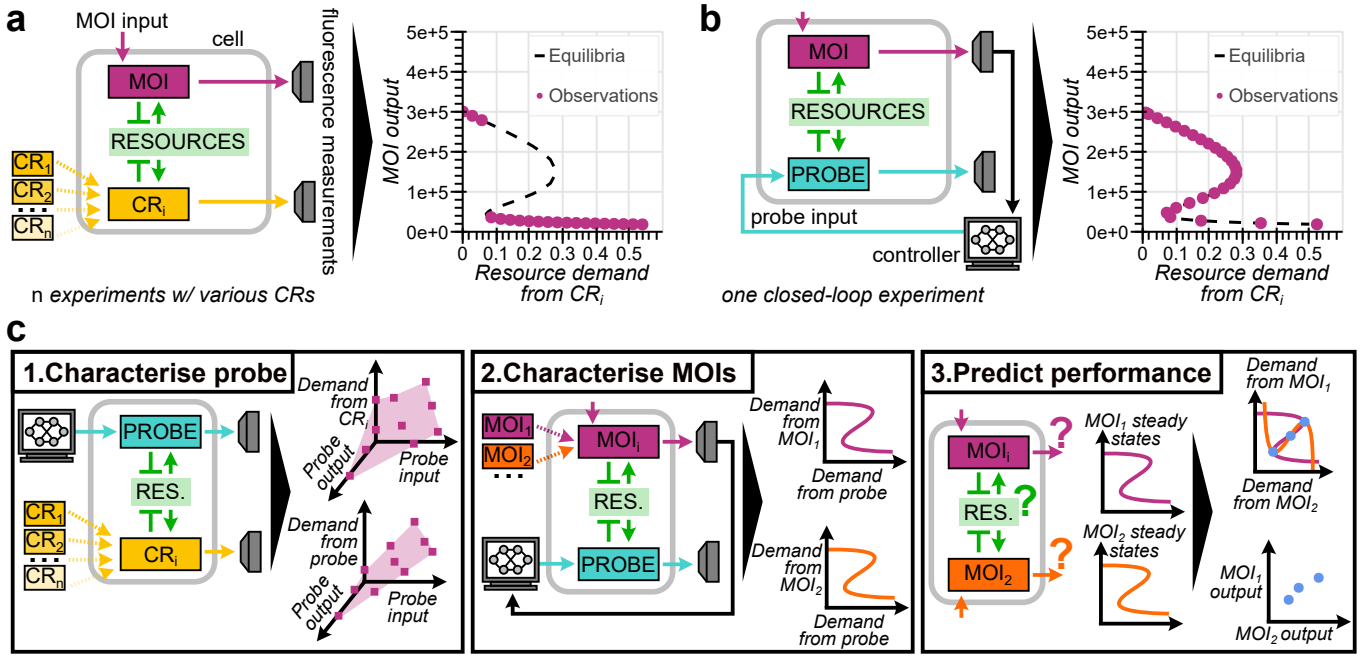

Fig. 1. Overview of the proposed method. (a) Conventional resource competition characterisation, requiring separate observations of a genetic module of interest (MOI) co-expressed with different constitutive reporters (CR), can fail to capture all possible steady states of the system. (b) CBC charcaterisation, in which the MOI's output is steered to different reference values by controlling resource competition in the cell via a co-expressed probe module, captures steady states all along the bifurcation curve. (c) Key steps of the proposed experimental protocol for characterising MOIs with CBC and predicting their steady-state outputs in the light of resource competition.

unstable steady states can be particularly difficult to capture in open-loop setups – as an unsteered system would diverge from them – yet be vital for predicting circuit behaviour, since they delimit the basins of attraction of different stable equilibria (e.g. representing different states of a memory device) [11]. Hence, reliably forecasting genetic modules' performance in relevant applications requires observing their multistability and bifurcations associated with resource competition. The impossibility of achieving this with extant experimental protocols therefore calls for the next generation of characterisation tools.

B. Circuit characterisation with feedback control

Here, we outline a blueprint for a novel experimental protocol that addresses the current limitations of resource competition characterisation methods for genetic modules. Instead of subjecting a module of interest to a constant resource demand created by a constitutive reporter in each experiment, our approach leverages a 'probe' module, the expression of whose genes is dynamically steered by a feedback control signal from an automated cell culture platform. This enables the use of control-based continuation (CBC), an emerging model-free testing algorithm recently extended to biological applications [7]. In CBC, stabilising feedback steers the system towards a steady state – even if it is normally unstable – allowing to observe it experimentally. By driving the plant through several equilibria in sequence, a bifurcation diagram revealing all of the system's steady states at different extents of resource competition can be obtained (Fig. 1b) [8], [13].

Our protocol for characetrising genetic modules and predicting their performance therefore involves three key components (Fig. 1c). First, a probe module with known competition properties is established. Second, a genetic module of interest (MOI) is characterised using this probe in a CBC setup. Third, resource demand bifurcation diagrams for different modules are combined to predict how they will behave in the same host cell as they compete for its resources.

In the rest of this paper, we provide a walkthrough of our proposed approach for the example of a self-activating genetic switch module, described using a basic resource-aware ODE model outlined in Section II and picked because its qualitatively resource-dependent steady-state behaviour has been observed experimentally [3] and leveraged in circuit design [12]. In Section III, all three steps of our protocol are performed *in silico*. Next, in Section IV we showcase our method's model-agnosticism by repeating the above steps for another, more complex resource-aware model of an engineered *E. coli* that considers different steps of gene expression separately, as well as capturing the host cell's metabolic regulation and protein precursor pool dynamics. Our method's implementability *in vivo*, potential limitations, and possible applications are discussed in Section V.

II. Model

A. Gene expression ODEs

Most simulations and derivations in this paper are performed using a basic model of a host *E. coli* cell expressing its native

genes and some synthetic genes added to it. Whilst heavily simplified for the sake of clarity and understandability of our protocol, this framework still incorporates key resource competition considerations of finite protein expression resources (most crucially for bacteria, ribosomes [6]) and constraints on the cell's total protein mass [1], [2], [14]. All of the cell's native genes are lumped into just two coarse-grained classes treated as a single gene – ribosomes r, which enable protein synthesis, and all other genes o. Together with the synthetic genes added to the cell, r and o comprise the set $\mathcal{S}$ of all genes being expressed. The concentration of gene $i \in \mathcal{S}$ proteins is denoted as p_i, and its dynamics is described by (1):

$$\dot{p}_i = \frac{\epsilon}{n_i} \cdot \frac{F_i(\cdot)q_i}{1+\sum_{j\in\mathcal{S}} F_j(\cdot)q_j} p_r - p_i \cdot \lambda(\{F_j\}_{j\in\mathcal{S}}, p_r) \quad (1)$$

Here, protein production is assumed to be a single-step reaction happening at the rate ϵ in amino acids per ribosome per hour, hence the need to divide it by the number n_i of amino acid residues in the protein chain. The factor at the total abundance of ribosomes p_r captures the fraction of resources allocated towards synthesising protein i, where q_i is its maximum possible resource demand and $0 \leq F_i(\cdot) \leq 1$ is the regulation function with gene-specific form and arguments. Neglecting native gene regulation mechanisms for simplicity, we postulate $F_r \equiv F_o \equiv 1$. The removal of proteins predominantly occurs by dilution as the cell grows and expands in volume at rate λ [1]. As protein mass density in the cell M is finite and constant [14], this rate of growth must equal the total rate of protein synthesis, which gives rise to (2):

$$\lambda(\{F_j\}_{j\in\mathcal{S}}, p_r) = \frac{\epsilon}{M} \cdot \frac{\sum_{j\in\mathcal{S}} F_j(\cdot)q_j}{1+\sum_{j\in\mathcal{S}} F_j(\cdot)q_j} p_r \quad (2)$$

A synthetic fluorescent protein must maturate before it can emit light [15]. For such genes, we thus separately consider the concentrations of nascent proteins p_i^n and mature proteins p_i^m, where the latter is the variable that can be experimentally observed in a microscope. The split ODE (1) for fluorescent proteins thus becomes ODEs (3a)–(3b), with μ_i being the maturation rate (note that $p_i = p_i^n + p_i^m$):

$$\dot{p}_i^n = \frac{\epsilon}{n_i} \cdot \frac{F_i(\cdot)q_i}{1+\sum_{j\in\mathcal{S}} F_j(\cdot)q_j} p_r - p_i^n \cdot \mu_i - p_i^n \cdot \lambda \quad (3a)$$

$$\dot{p}_i^m = p_i^n \cdot \mu_i - p_i^m \cdot \lambda \quad (3b)$$

B. Genetic modules

Besides the cell's native genes, in this paper we consider three kinds of synthetic gene circuit modules, shown in Fig. 2:

1) Constitutive reporters, used in conventional resource competition characterisation experiments. Such a module consists of a single unregulated gene c_i encoding a fluorescent protein whose emission we observe with a microscope. Hence, its regulation function is $F_{c_i} \equiv 1$, and its protein dynamics are given by ODEs (3a)–(3b).

2) Probe module, the expression of whose genes is steered by the controller to manipulate the extent of resource competition in the cell. The simplest instance of such control

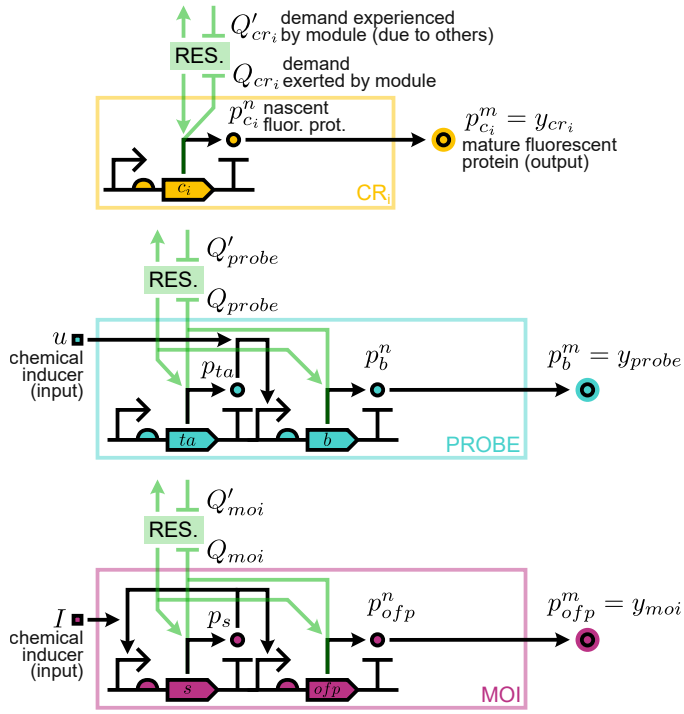

Fig. 2. Genetic modules considered in this study and described in Section II-B

is changing the concentration of the chemical inducer u in the culture medium supplied to the cells. This concentration modulates the activity of constitutively expressed transcription activator (ta) proteins which must be bound by an inducer in order to upregulate the expression of an output fluorescence protein b. The ta gene's expression is thus governed by ODE (1) and that of b by ODEs (3a)–(3b). Whilst $F_{ta} \equiv 1$, F_b is given by (4), which captures the binding between the inducer and the activator proteins with a half-saturation constant $K_{ta,i}$ and the cooperative binding between the inducer-activator complexes and the ofp gene's DNA with a half-saturation constant $K_{tai,b}$ and a Hill coefficient $\eta_{tai,b}$. In absence of activators, the ofp gene exhibits low baseline expression $F_{b,0}$.

$$F_b(u, p_{ta}) = \frac{F_{b,0} K_{tai,b}^{\eta_{tai,b}} + \left(\frac{u}{u+K_{ta,i}} p_{ta}\right)^{\eta_{tai,b}}}{K_{tai,b}^{\eta_{tai,b}} + \left(\frac{u}{u+K_{ta,i}} p_{ta}\right)^{\eta_{tai,b}}} \quad (4)$$

3) Module of interest (self-activating genetic switch), comprising a switch gene s and an output fluorescent protein gene ofp, whose protein dynamics are respectively given by ODE (1) and ODEs (3a)–(3b). Like ta, s is a transcription activator. However, it is bound by a different inducer whose concentration remains unchanging throughout the experiment, so the fraction of inducer-bound switch proteins is a constant I. As it is self-activating, the switch upregulates both its own and protein b's synthesis. We thus have (5) with $K_{s,s}$, $\eta_{s,s}$ and $F_{s,0}$ being analogous to the corresponding parameters in (4):

$$F_s(p_s) = F_{ofp}(p_s) = \frac{F_{s,0} + (Ip_s)^{\eta_{s,s}}}{K_{s,s}^{\eta_{s,s}} + (Ip_s)^{\eta_{s,s}}} \quad (5)$$

C. Notation for module resource demands and outputs

Let the cell host two genetic modules with gene sets $\mathcal{M}_1$ and $\mathcal{M}_2$ respectively, so $\mathcal{S} = \{r, o\} \cup \mathcal{M}_1 \cup \mathcal{M}_2$. Our experimental protocol focusses on characterising and predicting resource competition between such two synthetic genetic modules in the steady state. It is thus convenient to abstract the host cell's own genes by normalising steady-state resource demands to those of the native genes in (6), where the bar signifies equilibrium values:

$$Q_i = \frac{\overline{F}_i(\cdot) q_i}{q_r + q_o} = \overline{F}_i(\cdot) Q_i^{max} \tag{6}$$

For a given module, it is also useful to consider the total resource demand that all of its genes *exert* on the cell, as well as the total demand it *experiences* due to the other module. For the first module, these quantities are respectively given by $Q_{1,t}$ and $Q'_{1,t}$ in (7). Meanwhile, since the demand exerted by one module is experienced by the other, for the second module we will have $Q_{2,t} = Q'_{1,t}$ and $Q'_{2,t} = Q_{1,t}$.

$$Q_{1,t} = \sum_{j \in \mathcal{M}_1} Q_j \quad \text{and} \quad Q'_{1,t} = \sum_{j \in \mathcal{M}_2} Q_j \tag{7}$$

What are the steady-state observations which can be made for the cells expressing a given pair of modules? First, there are these modules' corresponding outputs $\overline{y}_{1,1+2}$ and $\overline{y}_{2,1+2}$, i.e. the levels of mature output fluorescent proteins, whose emission is observed by a microscope. Second, the cell growth rate $\overline{\lambda}_{1+2}$ is measurable as the rate of change of cell length in microscopy images [10]. For reference, a module can also be observed alone in the host cell, without any competitors – this, for example, gives rise to output $\overline{y}_{1,1}$ and growth rate $\overline{\lambda}_1$ for module 1. Comparing this to the case of two competing modules, the ratio of output protein expression can be calculated according to (8), where the output protein maturation rate μ_1 is assumed to be known from literature [15] or prior experiments.

$$\rho_{1,1+2} = \frac{(\overline{\lambda}_{1+2} + \mu_1)\overline{y}_{1,1+2}}{(\overline{\lambda}_1 + \mu_1)\overline{y}_{1,1}} \tag{8}$$

III. Protocol walkthrough

A. Probe characterisation

Since a genetic module of interest's resource competition properties are originally unknown, observing them in a CBC experiment requires gauging them from the inputs and outputs of the probe module co-expressed with it. Importantly, we need to evaluate not only the resource demand $Q_{moi,t} = Q'_{probe,t}$ exerted by the MOI on the probe, but also the demand $Q'_{moi,t} = Q_{probe,t}$ exerted by the probe on the MOI, which may vary as resource availability changes affect the interactions between the probe's constituent genes. Whilst the Appendix proves that this can indeed be done unambiguously, such determination of resource demands still requires the probe's own resource competition properties to be known first.

This can be achieved using constitutive reporter assays. First, a library of n constitutive reporters is established

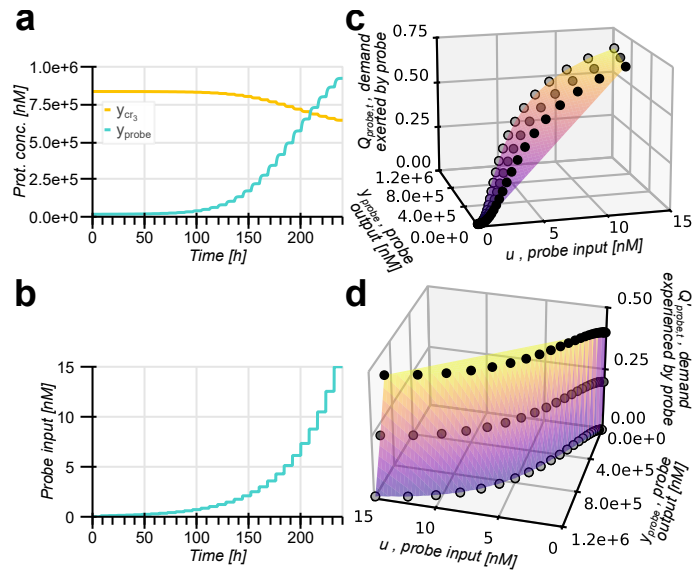

Fig. 3. Simulation of probe module characterisation with $n = 3$ constitutive reporters and $m = 16$ chemical inputs. (a–b) System trajectory during the parameter sweep with the highest-demand reporter cr_3. (c–d) Obtained sample data points (black) and linear interpolations of the mappings $\mathcal{B}_{Q'}$ and $\mathcal{B}_Q$ mathcing the probe's input-output pairs to the resource demand it experiences and exerts on other modules. Darker points stand for measurements with higher-demand constitutive reporters.

likewise to the steps described in [2]. Since each of them comprises a single unregulated gene, their resource demands $\{Q_{cr_i,t}\}$ are always the same and can be estimated according to (9) by first expressing each reporter alone in the cell, then by observing a pair of reporters cr_i and cr_j together in the host cell:

$$Q_{cr_i,t} = \frac{1 - \rho_{cr_j, cr_i + cr_j}}{\rho_{cr_i, cr_i + cr_j} + \rho_{cr_j, cr_i + cr_j} - 1} \tag{9}$$

Once a library of known constitutive reporters has been created, we perform an open-loop experiment in which the probe is expressed with each of the reporters, sweeping through m inputs and recording the resultant fluorescent outputs. As a result, we obtain $n \times m$ steady-state observations, for which we record 1) the probe input $\overline{u}$, 2) the probe output $\overline{p}_b^m$, 3) the resource demand experienced by the probe $Q'_{probe,t} = Q_{cr_i,t}$ and 4) the resource demand exerted by the probe, calculated from the constitutive reporter's output as:

$$Q_{probe,t} = \frac{(1 + Q_{cr_i,t})(1 - \rho_{cr_i, cr_i + probe})}{\rho_{cr_i, cr_i + probe}} \tag{10}$$

These data points represent samples from the mappings $\mathcal{B}_{Q'} : (u, \overline{y}_{probe}) \to Q'_{probe,t}$ and $\mathcal{B}_Q : (u, \overline{y}_{probe}) \to Q_{probe,t}$ that match the probe's input-output pairs to the resource demands experienced and exerted by it. For inputs and/or outputs between the sampled points, $Q'_{probe,t}$ and $Q_{probe,t}$ can be interpolated from the samples. In CBC characterisation, these mappings will be used to gauge resource competition in the cell from the probe's input-output behaviour.

To illustrate this mapping generation process, we simulate it as shown in Fig. 3. For this and all other simulations, model

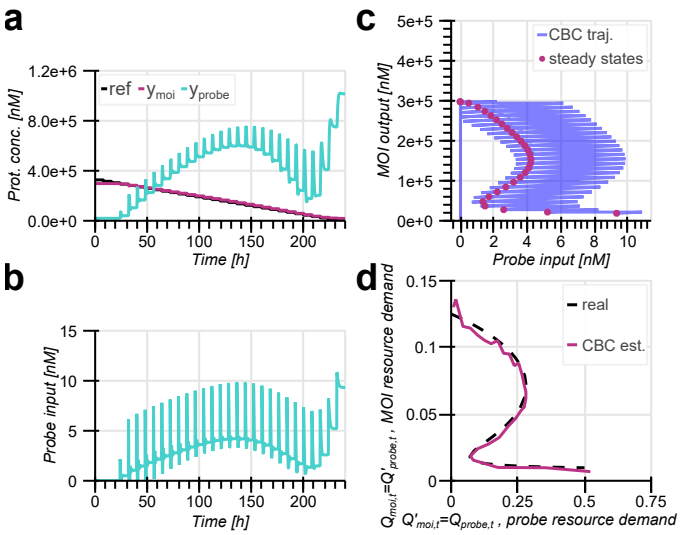

Fig. 4. Simulation of MOI characterisation with CBC. (a–b) CBC trajectory with the proportional control law $u = K_p(y_{moi} - R)$. Transient spikes in u and y_{probe} correspond to switching to a new reference, which sharply increases the error, and decay as the new steady state is approached. (c) Obtained CBC bifurcation curve relating the steady-state input of the probe to the output of the MOI competing with it for resources. (d) Dashed: resource demand bifurcation curve $\mathcal{C}_{moi}$ relating the steady-state resource demands experienced and exerted by the characterised MOI, retrieved analytically according to (12). Solid: $\mathcal{C}_{moi}$ estimated from experimental data by applying the $\mathcal{B}_{Q'}$ and $\mathcal{B}_Q$ mapping to the CBC trajectory.

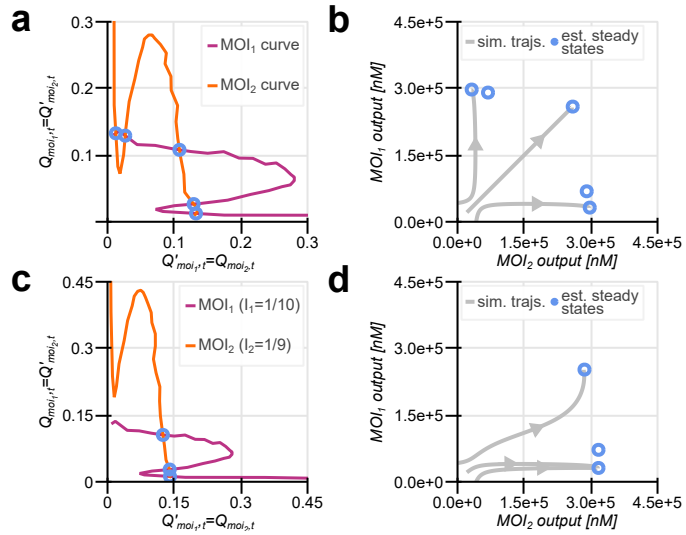

Fig. 5. Using characterisation outcomes to predict steady states of identical self-activating genetic switch modules competing for the cell's resources. (a) Intersections between the superimposed estimated resource demand curves $\mathcal{C}_{moi_1}$ and $\mathcal{C}_{moi_2}$ reveal possible steady states of the overall system. (b) Circles: module outputs corresponding to the identified system steady states. Lines: simulated trajectories of the two-switch systems converging close to the identified steady states' estimated outputs. (c–d) Steady-state prediction repeated for the case when the second switch is induced with $I = \frac{1}{9}$ as opposed to $I = \frac{1}{10}$ for the first switch here and both switches in a–b.

parameters and implementation in Python can be found at https://github.com/KSechkar/CoBa_CRAB.

B. Module of interest characterisation with CBC

To characterise a given module of interest, we put it into the same cell as the probe and perform a CBC experiment. Namely, the output $y_{moi} = p^m_{moi}$ is steered towards a reference R by a control signal u until both y_{moi} and u reach constant values (Fig. 4a–b). The observations at this point correspond to an open-loop system's steady-state, regardless of whether it was originally stable or unstable (and therefore difficult to capture). By making the system track m references $R_1, R_2, \dots R_m$ one after another, a comprehensive view of its steady states can be obtained [7], [8], [13].

This produces a CBC bifurcation curve, whose points $\{(\overline{u}, \overline{y}_{moi})|_{R=R_i}\}$ reveal the system's steady-state input-output combinations. If for each captured steady state we also record the probe outputs $\{\overline{y}_{probe}|_{R=R_i}\}$, the mappings $\mathcal{B}_{Q'}$ and $\mathcal{B}_Q$ allow to translate the captured bifurcation curve into a resource demand bifurcation curve $\mathcal{C}_{moi}$ whose points

$$\left\{\left(Q'_{moi,t}, Q_{moi,t}\right) = \left(\mathcal{B}_{Q'}(\overline{u}, \overline{y}_{probe}), \mathcal{B}_Q(\overline{u}, \overline{y}_{probe})\right)|_{R=R_i}\right\} \tag{11}$$

relate the resource demands experienced and exerted by the module in the steady state. In Fig. 4d, it can be seen that the estimates obtained by CBC characterisation closely follow the real resource demand bifurcation curve, which is determined by analytically solving $\dot{p}_s = 0$ to obtain:

$$Q'_{moi} = \frac{Q^2_{moi}\left(M\overline{F}_s - \overline{p}_s\right)}{(Q^{max}_s + Q^{max}_{ofp})\overline{p}_s} - 1, \text{ where} \tag{12a}$$

$$\overline{p}_s = \frac{K_{s,s}}{I}\left(\frac{\overline{F}_s - F_{s,0}}{\overline{F}_s - 1}\right)^{\eta^{-1}_{s,s}}, \overline{F}_s = \frac{Q_{moi}}{Q^{max}_s + Q^{max}_{ofp}} \tag{12b}$$

C. Prediction of resource competition between modules

How can one predict the steady-state behaviour of two modules moi_1 and moi_2 hosted by the same cell, provided that they have been characterised with CBC as per Section III-B? Let us recall that the resource demand exerted by one module is experienced by the other (and vice versa), so $Q_{moi_1,t} = Q'_{moi_2,t}$ and $Q'_{moi_1,t} = Q_{moi_2,t}$. Hence, it is possible to plot the two resource demand bifurcation curves $\mathcal{C}_{moi_1}$ and $\mathcal{C}_{moi_2}$ on the same axes. For the overall system to be in steady state, both modules must be in their respective equilibria given by their bifurcation curves. Hence, the possible steady states of the combined gene expression system are given by intersections between $\mathcal{C}_{moi_1}$ and $\mathcal{C}_{moi_2}$. By mapping these intersections from resource demands back onto MOI outputs, the modules' possible output combinations can be retrieved. Notably, neither the bifurcation curve's retrieval nor the output prediction step assume any prior knowledge of the MOIs' architecture or properties and solely rely on experimental measurements.

The predictive power of our method is confirmed by simulation in Figure 5, where the simulated trajectories of

two self-activating genetic switches converge from different initial conditions towards the possible output combinations which correspond to intersections between resource demand bifurcation curves. Importantly, our protocol may not merely help to estimate the steady-state outputs, but also allow to spot qualitative changes in a system's steady-state performance. For instance, repeating the CBC procedure from Section III-B for a switch with greater chemical induction produces a shifted resource demand bifurcation curve $\tilde{\mathcal{C}}_{moi_2}$ which has fewer intersections with $\mathcal{C}_{moi_1}$ in Fig. 5c. This is consistent with the system having fewer possible steady-state outputs as shown in Fig. 5d.

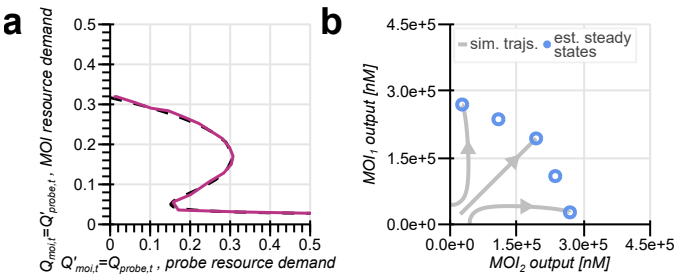

Fig. 6. Simulation of the CBC characterisation and steady state prediction protocol with a coarse-grained mechanistic resource-aware cell model, for the example of a self-activating genetic switch module. (a) Real resource demand bifurcation curve $\mathcal{C}_{moi}$ (dashed; retrieved analytically as per [12]) and its estimate obtained by CBC characterisation (solid), analogous to Fig 4d. (b) Steady-state outputs of two self-activating switches competing for the cell's resources as predicted from CBC characterisation results (circles) and simulated trajectories of such a two-switch system converging to the identified steady states (lines), analogous to Fig 5b. Note that the exact curve shape and outputs are different due to another model with different parameters being considered.

IV. Protocol Extension to a Complex Resource-Aware Cell Model

Our protocol's characterisation of genetic modules in Section III-B is based on CBC, whose model-free nature makes it suitable for studying systems with potentially unknown dynamics [7], [8], [13]. Likewise, in Section III-A knowledge of the probe module's dynamics is not required, as the mappings $\mathcal{B}_{Q'}$ and $\mathcal{B}_Q$ capturing the probe module's resource competition properties are reconstructed simply by interpolation between experimentally acquired data points. Meanwhile, although our translation of probe inputs and outputs into resource demands in Section III-A does assume a Hill dependence of protein expression rates on resource competition captured by the demands $\{Q_i\}$, this relation is not arbitrary. Rather, it is both mechanistically explained by competitive gene expression machinery binding dynamics and represents an empirical observation, which different resource-aware models with widely ranging starting assumptions are defined to reproduce [1], [2], [5], [6].

Our approach can thus be considered model-agnostic as long as the tested system's properties are consistent with resource competition patterns commonly observed across various experiments and even different model organisms [1], [2], [4]–[6].

To illustrate this, in Fig. 6 we simulate the application of our method to a different, more complex modelling framework than the one considered in Sections II–III. Namely, we adopt a coarse-grained resource-aware mechanistic cell model from [1], originally implemented in Python for [16] with efficient computation enabled by the JAX package [17]. This framework explicitly considers different steps of gene expression (rather than treating it as a single reaction in (1)), as well as captures dynamic regulation of ribosome synthesis and nutrient metabolism [1]. Despite the model's qualitatively increased complexity, Fig. 6 shows that our method still gives rise to correct predictions, which supports its promise of *in vivo* applicability to more complex real biological systems that may involve unknown interdependencies between our measured and actuated parameters.

V. Conclusion

In summary, we have described and simulated a novel experimental method which applies automatic feedback control to the problem of characterising a synthetic gene circuit module's resource competition properties. Designed to provide a more complete and informative view of module behaviour than the extant open-loop experimental approaches, our protocol allows to reliably predict steady-state behaviours of two genetic modules competing for the same host cell's resources.

Our work contributes to a growing body of experimental methods that aim to overcome the limitations of conventional biological laboratory techniques by combining microscopy, real-time single-cell control, and computational methods in order to optimise the experimental design for maximum informativeness [10], [18] and observe difficult-to-capture cell behaviours [7], [9]. Hence, our proposed approach is well-positioned to leverage the emerging tools in synthetic biology, automated cell culturing, and control engineering developed to enable these novel experimental methods. This can help to overcome potential hurdles on the way to the practical implementation and widespread adoption of our protocol – most prominently, the requirement of long experimental timescales (e.g. bifurcation curve acquisition takes $240\ h$ in our case, characteristically for CBC applied to biology [7]), as well as the need for robustness to intercellular variability and noisy measurements and gene expression dynamics.

Our CBC approach's flexibility and model-agnosticism make it particularly easy to incorporate and combine the advantages of different experimental tools. Namely, a wide range of control strategies can be used to calculate feedback signals for CBC. Hence, more advanced solutions like model-predictive control, rather than the simple proportional feedback controller tracking each reference for a fixed time (which we deploy in this work), have been shown to accelerate experimental data collection and improve robustness to noise [7]. Meanwhile, the automated cell culture platform suggested for implementing CBC experiments practically – and validated *in silico* using agent-based simulations – is a microfluidic chip with individual bacterial cells at the end of each of thousands of trenches [7]. This setup can be made particularly powerful

by applying control signals individually to each cell in a chip, e.g. using light to steer an optogenetically controlled probe module as opposed to chemical inputs affecting all bacteria growing in the medium [10]. Simultaneously acquiring thousands of CBC trajectories, steered by control signals computed in an efficient and parallelised manner [10], [16], [17], can enable reliable population-average measurements despite individual trajectories' stochasticity, as well as accelerate the acquisition of experimental measurements, e.g. by using different subsets of cells to capture different sections of the resource demand bifurcation curve. Focussing on genetic modules' general resource competition properties, rather than a particular system's characteristic, our method leaves the choice of a CBC probe module rather unconstrained as long as its input-output responses are reflective of resource competition in the cell. Even if this property may not always be theoretically proven (like we do for a chemically controlled probe in the Appendix), it may still be established experimentally by testing different optogenetic tools from the wide range developed by synthetic biologists [19].

Even with such improvements in efficiency, a CBC experiment would be more involved and resource-intensive than a simpler setup. This, however, is offset by the reusability of its results. A once-characterised probe can be deployed in CBC testing of many different modules. Furthermore, once a resource demand bifurcation diagram for a module is obtained, it can be used to make predictions about its behaviour alongside any other module characterised in the same manner. As CBC testing is performed for more modules, it usefulness and predictive power will thus scale combinatorially.

This promises to significantly facilitate the development of reliable modular genetic circuits acting as biomolecular sensors or memory devices, where input-output responses must be known despite any resource availability fluctuations [11]. Another application likely to benefit from our method is cell fate reprogramming, in which competition between genetic regulators can qualitatively alter their behaviour and convergence upon one of several possible steady-states [3]. Moreover, resource-dependent bifurcations, which our analysis helps to establish, have recently themselves been leveraged in the design of biomolecular controllers aimed at increasing the evolutionary stability of biotechnologies [12].

Appendix

We assume no knowledge of the module of interest's properties, so all resource competition interactions in the cell must be estimated from observing the probe module described in Section II-B. The probe's inputs $\{u\}$ are known as they are calculated and recorded on a computer and fluorescence outputs $\{\overline{y}_{probe} = \overline{p}_b^m\}$ are measured with a microscope (Fig. 1b). *Theorem 1*, which follows from *Lemma 1*, proves that these values allow to unambiguously determine the resource demands of all genetic modules present in the cell.

Lemma 1: For a given input $\overline{u}$ and resource demand $Q'_{probe,t}$ experienced by the probe module, exactly one steady-state output gene regulation function value $\overline{F}_b(\overline{u}, Q'_{probe,t})$ is possible. Moreover, for a given $\overline{u}$ there are no such two values $Q'_{probe,t} \neq \tilde{Q}'_{probe,t}$ that $\overline{F}_b(\overline{u}, Q'_{probe,t}) = \overline{F}_b(\overline{u}, \tilde{Q}'_{probe})$.

Proof: Recalling that F_b is a function of u and p_{ta} as per (4), let us express p_{ta} in terms of the steady-state $\overline{F}_b$ and $\overline{u}$, substitute it into $\dot{p}_{ta} = 0$, and rearrange the terms to get (13):

$$0 = \phi_{Q'_{probe,t}}(\overline{F}_b) = \left(\frac{K_{tai,b}(u + K_{ta,i})(\overline{F}_b - \overline{F}_{b,0})}{u(1 - \overline{F}_b)}\right)^{\eta_{tai,b}^{-1}} \times \\ \times \left(1 + Q'_{probe,t} + Q_{ta}^{max} + \overline{F}_b Q_b^{max}\right) - Q_{ta}^{max} \quad (13)$$

According to (4), F_b only takes values between $F_{b,0}$ and 1. Since all parameters for biochemical systems like ours are non-negative, we note that $\phi_{Q'_{probe,t}}(\overline{F}_b) = -Q_{ta}^{max}$, $\lim_{\overline{F}_b \to 1} \phi_{Q'_{probe,t}}(\overline{F}_b) = +\infty$, and $d\phi_{Q'_{probe,t}}/d\overline{F}_b > 0$. Rising monotonically from a negative to a positive infinite value, the continuous function $\phi_{Q'_{probe,t}}$ must therefore have exactly one root for which $\phi(\overline{F}_b) = 0$. Then, let us observe that for $Q'_{probe,t} \neq \tilde{Q}'_{probe,t}$ and any $\overline{F}_b > F_{b,0}$, we have $\phi_{Q'_{probe,t}}(\overline{F}_b) \neq \phi_{\tilde{Q}'_{probe,t}}(\overline{F}_b)$. Hence, the roots of the two functions must be different. □

Theorem 1: The steady-state resource demands experienced by the probe due to competing genetic modules, as well as the demand exerted by the probe, can be unambiguously determined from its input and output. That is, there exist bijecions $\mathcal{B}_{Q'} : (\overline{u}, \overline{y}_{probe}) \to Q'_{probe,t}$ and $\mathcal{B}_Q : (\overline{u}, \overline{y}_{probe}) \to Q_{probe,t}$.

Proof. Set $\dot{p}_b^m = 0$ and $\dot{p}_r = 0$, then recall (2) to get:

$$\overline{p}_b^m = \frac{\mu_b}{\mu_b + \overline{\lambda}} \cdot \frac{M}{n_b} \cdot \frac{\overline{F}_b Q_b^{max}}{\overline{F}_b Q_b^{max} + Q'_{probe,t} + Q_{ta} + 1} \quad (14a)$$

$$\overline{\lambda} = \frac{\epsilon \overline{p}_r}{M} \cdot \frac{\overline{F}_b Q_b^{max} + Q'_{probe,t} + Q_{ta} + 1}{\overline{F}_b Q_b^{max} + Q'_{probe,t} + Q_{ta} + 1 + \frac{1}{q_r + q_o}} \quad (14b)$$

$$\overline{p}_r = \frac{M}{n_r} \cdot \frac{q_r/(q_r + q_o)}{\overline{F}_b Q_b^{max} + Q'_{probe,t} + Q_{ta} + 1} \quad (14c)$$

According to (14), for $F_{b,0} \leq \overline{F}_b \leq 1$ we have $\frac{d\overline{\lambda}}{d\overline{F}_b} < 0$ and thus $\frac{d\overline{p}_b^m}{d\overline{F}_b} > 0$. Consequently, $\overline{p}_b^m$ rises monotonically from the lowest-possible to the greatest-possible steady-state output value as $\overline{F}_b$ increases. Hence, there is a one-to-one match between the output gene's steady-state regulatory function and its measured mature protein concentration. Combined with *Lemma 1*, this means that for a given input $\overline{u}$, there can be no such two values $Q'_{probe,t}$ and $\tilde{Q}'_{probe,t}$ for which $(\overline{u}, Q'_{probe,t})$ and $(\overline{u}, \tilde{Q}'_{probe,t})$ give rise to the same probe output $\overline{y}_{probe} = \overline{p}_b^m$, so $\mathcal{B}_{Q'}$ is a bijection. Then, due to *Lemma 1* the resource demand exerted by the probe is matched to the input-output pair via (15), making $\mathcal{B}_Q$ a bijection as well. □

$$Q_{probe,t} = Q_{ta}^{max} + Q_b^{max} \overline{F}_b(\overline{u}, \mathcal{B}_{Q'}(\overline{u}, \overline{y}_{probe})) \quad (15)$$

Acknowledgment

We thank Sara Brancato, Prof. Lucia Marucci and Dr Ludovic Renson for insightful discussions.

References

[1] K. Sechkar, H. Steel, G. Perrino, and G.-B. Stan, "A coarse-grained bacterial cell model for resource-aware analysis and design of synthetic gene circuits," *Nature Communications*, vol. 15, no. 1, p. 1981, 2024.

[2] Y. Qian, H.-H. Huang, J. I. Jiménez, and D. Del Vecchio, "Resource competition shapes the response of genetic circuits," *ACS Synth. Biol.*, vol. 6, no. 7, pp. 1263–1272, 2017.

[3] R. Zhang, H. Goetz, J. Melendez-Alvarez, *et al.*, "Winner-takes-all resource competition redirects cascading cell fate transitions," *Nat. Commun.*, vol. 12, no. 1, 2021.

[4] C. D. McBride and D. Del Vecchio, "Predicting composition of genetic circuits with resource competition: Demand and sensitivity," *ACS Synth. Biol.*, 2021.

[5] T. Frei, F. Cella, F. Tedeschi, *et al.*, "Characterization and mitigation of gene expression burden in mammalian cells," *Nature Communications*, no. 1, 2020.

[6] A. Gyorgy, José, J. Yazbek, *et al.*, "Isocost lines describe the cellular economy of genetic circuits," *Biophysical Journal*, vol. 109, no. 3, pp. 639–646, 2015.

[7] I. de Cesare, D. Salzano, M. di Bernardo, L. Renson, and L. Marucci, "Control-based continuation: A new approach to prototype synthetic gene networks," *ACS Synthetic Biology*, vol. 11, no. 7, pp. 2300–2313, 2022.

[8] S. Beregi, D. A. W. Barton, D. Rezgui, and S. A. Neild, "Robustness of nonlinear parameter identification in the presence of process noise using control-based continuation," *Nonlinear Dyn.*, vol. 104, no. 2, pp. 885–900, 2021.

[9] D. Choudhary, K. R. Foster, and S. Uphoff, "Chaos in a bacterial stress response," *Current biology : CB*, vol. 33, no. 24, p. 5404, 2023.

[10] R. Chait, J. Ruess, T. Bergmiller, G. Tkačik, and C. C. Guet, "Shaping bacterial population behavior through computer-interfaced control of individual cells," *Nature Communications*, vol. 8, no. 1, 2017.

[11] A. Gyorgy, "Context-dependent stability and robustness of genetic toggle switches with leaky promoters," *Life*, no. 11, p. 1150, 2021.

[12] K. Sechkar and H. Steel, "Model-guided gene circuit design for engineering genetically stable cell populations in diverse applications," *J. R. Soc. Interface*, vol. 22, no. 223, 2025.

[13] J. Sieber and B. Krauskopf, "Control based bifurcation analysis for experiments," *Nonlinear Dynamics*, vol. 51, no. 3, pp. 365–377, 2008.

[14] M. Basan, M. Zhu, X. Dai, *et al.*, "Inflating bacterial cells by increased protein synthesis," *Mol. Syst. Biol.*, vol. 11, no. 10, p. 836, 2015.

[15] E. Balleza, J. M. Kim, and P. Cluzel, "Systematic characterization of maturation time of fluorescent proteins in living cells," *Nature Methods*, vol. 15, no. 1, pp. 47–51, 2018.

[16] O. Gallup, K. Sechkar, S. Towers, and H. Steel, "Computational synthetic biology enabled through jax: A showcase," *ACS Synth. Biol.*, vol. 13, no. 9, 2024.

[17] J. Bradbury, R. Frostig, P. Hawkins, *et al.*, *JAX: Composable transformations of Python+NumPy programs*, version 0.4.23, 2023. [Online]. Available: http://github.com/google/jax.

[18] M. Kryukov, A. Carcano, G. Batt, and J. Ruess, "Can optimal experimental design serve as a tool to characterize highly non-linear synthetic circuits?" In *2019 18th European Control Conference (ECC)*, 2019, pp. 1176–1181.

[19] M. Benisch, S. K. Aoki, and M. Khammash, "Unlocking the potential of optogenetics in microbial applications," *Curr. Opin. Microbiol.*, vol. 77, p. 102 404, 2024.